23rd ABCM International Congress of Mechanical Engineering
December 6-11, 2015, Rio de Janeiro, RJ, Brazil

EFFECT OF COOLING RATE AFTER HEAT TREATMENT AT HIGH TEMPERATURE IN THE LOCALIZED CORROSION OF UNS S31803 STEEL

Davi Pereira Garcia
Instituto Federal do Espírito Santo, Rua Duque de Caxias, 194A, Carapina, São Mateus - ES CEP 29933-030
davi.garcia@ifes.edu.br
Marcelo Camargo Severo de Macedo
Universidade Federal do Espirito Santo UFES, Av. Fernando Ferrari, 514, Goiabeiras, Vitória - ES - CEP 29075-910
mcamargo0207@gmail.com
Sergio Souto Maior Tavares Second Author's Name
Universidade Federal Fluminense, Rua Passo da Pátria, 156 – São Domingos, Niterói - RJ CEP 24210-240
ssmtavares@terra.com.br

Abstract. *Duplex Stainless Steel have both phases ferrite and austenite in his microstructure in almost equal proportions, allowing it to have great strength corrosion and mechanical resistance. When exposed to high temperatures they are subject to microstructural changes making his properties to be modified.*
In this work localized corrosion resistance of the duplex stainless steel UNS S31803 heat treated by high temperature (1300◦C) for 30 minutes followed by different cooling rates is studied. Some samples were solution treated at 1000◦C for 1 hour and fast cooled after the high temperature treatment. A wide range of microstructures, with differents morphologies and phase proportions, were obtained by this way, also this microstructural changes during cooling process have promoted the precipitation of deleterious phases such as nitrides and sigma, making the corrosion strength to be altered.

Keywords: *Duplex Stainless Steel UNS S31803, High temperature heat treatement, cooling rates, deleterious phases, DL-EPR, Potentiodynamic Polarization*

1. INTRODUCTION

Featuring excellent mechanical strength and corrosion especially in aggressive media, the duplex stainless steels (DSS) have the microstructure containing roughly the same proportion of ferrite and austenite, and its properties depends of the relations between this phases(POHL et al., 2007; COBB, 2010). The DSS have been increasingly used in components of nuclear plants, chemical and petrochemical industries, and in other various engineering applications due their good mechanical properties, corrosion resistance and weldability (VIJAYALAKSHMI et al., 2011).

Research are being conducted to verify the behavior of these alloys when exposed to several cooling rates, because their original properties can be changed due to precipitation of tertiary phases, which can be beneficial or harmful for them.(GHOSH; MONDAL, 2008). At the temperature of 1300 ºC, the problem can be avoided by decreasing cooling rate, controlling the heat of the welding and with a proper preheating of the DSS welded. However, the cooling rate should be high enough to prevent the appearance of sigma phases, precipitation of chromium carbide and α' at temperatures between 350-1000 °C. (TAVARES et al., 2005)

In this work corrosion tests were made with electrochemical techniques of potentiodynamic reactivation double-loop (DL-EPR) and potentiodynamic polarization for analysis of stainless steel corrosion properties UNS S31803 treated to 1300 ° C and cooled in different conditions in order to obtain different phase ratios in the samples, furthermore, it was made annealing heat treatment at 1000 ° C in each sample in order to equalize the phase proportions again. Optical microscopy (OM) and scanning electron microscopy (SEM) were done in each sample after the tests in order to assess which phases have been suffered corrosion.

2. EXPERIMENTAL

The DSS UNS S31803 analyzed in this work (composition shown in Table 1) was received in 4 mm plates. In the condition without heat treatment had the microstructure consists of austenite of 55% (45% ferrite) (TAVARES et al., 2005). W—water cooling to room temperature (RT); O—oil cooling to RT; A— air-cooling to RT; FA—cooling into furnace till 1000◦C followed by air cooling to RT; and F—cooling into furnace to RT. After the high temperature treatment, some samples were solution treated at 1000◦C and water-cooled. Table 2 presents all heat treatment conditions produced.

Table 1 - Chemical composition (weight percentage) DSS UNS S31803

%Cr	%Ni	%Mo	%N	%C (máx.)	%Si (máx.)	%Mn (máx.)
22,5	5,74	3,2	0,16	0,018	0,35	1,42

Table 2- Heat treatments and samples identification.

Sample	Heat Treatments
W1	1300◦C, water cooling to room temperature (RT)
W2	same as W1 plus solution treatment (1000◦C/1 h, water cooling)
O1	1300◦C oil cooling to RT
O2	same as O1 plus solution treatment (1000◦C/1 h, water cooling)
A1	1300◦C air cooling to RT
A2	same as A1 plus solution treatment (1000◦C/1 h, water cooling)
FA1	1300◦C furnace cooling to 1000◦C, air cooling to RT
FA2	same as FA1 plus solution treatment (1000◦C/1 h, water cooling)
F1	1300◦C furnace cooling to RT
F2	same as F1 plus solution treatment (1000◦C/1 h, water cooling)

The purpose of cooling at different temperatures was to obtain samples having different microstructures. Was analyzed the percentage of austenite present after each heat treatment, and found that the samples had the austenite percentages as shown in Table 3. (TAVARES et al., 2005)

Table 3 - Amount of austenite in each sample (TAVARES et al., 2005).

Sample	% ϒ	Sample	% ϒ
W1	17,1 ± 4,1	W2	59,8 ± 3,6
O1	27,6 ± 3,7	O2	58,6 ± 4,2
A1	39,7 ± 9,6	A2	58,0 ± 11,0
FA1	55,4 ± 5,0	FA2	59,8 ± 12
F1	60,5 ± 12	F2	56,3 ± 7,8

For the corrosion tests, incoming samples were cut into 29 x 13 x 4 mm. After performing the cutting of which samples they were built in acrylic resin and connected to a wire for closing the circuit with the potentiostat so the tests could be performed.

Tests were performed using DL-EPR to evaluate the susceptibility to intergranular corrosion (LOPEZ et al., 1997). These tests were performed with a three-electrode electrochemical cell, a Pt electrode as an auxiliary, a saturated calomel electrode (SCE) as the reference and the working electrodes were built with samples that were prepared in 500 grain size sandpaper and a demarcated area in 0,28 cm^2. The tests were performed three times where it had beginning at the open circuit potential (OCP) obtained after immersing the sample for 30 min followed by scanning toward the anode at a rate of 1.67 mV/s until a potential of 750 mV higher than the OCP were measured. After reaching this potential a reverse bias in the cathodic direction was made until the OCP again. The solution used was 2M H_2SO_4 + 0,01M KSCN + 0,5M NaCl (PARDAL et al., 2013). The sensitization was measured by the ratio Ir/Ia where Ia is the peak current of

the anodic activation polarization and Ir is the peak current in the reactivation reverse scan. To evaluate this susceptibility to intergranular corrosion an AUTOLAB PGSTAT potentiostat was used.

For the tests to evaluation pitting corrosion, ASTM G61-83 was consulted (ASTM, 2003). The potentiodynamic polarization test was done in samples that had their areas delimited on 0,28 cm2, the scan rate was 1 mV.s-1. After immersion of an 1 hour and measuring the OCP, the scan was performed only in the anodic direction and continued until the current of 5mA/cm2 it was reached and the data plotted on on a logarithmic scale graph. The solution used in this tests was 3,5%NaCl. The samples were ground to # 800 and the experiment was carried out at 24 °C with a AUTOLAB PGSTAT potentiostat. Microstructural characterization of the samples corrosion tested were made with SEM and MO and also was performed with an electrolytic attack using a solution of 10% oxalic 3V for 180 s.

3. RESULTS

Figure 1- 5 show micrographs of the samples treated at 1300 ° C and cooled in differents ways. W1 and O1 samples are observed the presence of nitrides, these are formed due to the fastest cooling rate that these samples were imposed. In the sample A1 the austenite grains begin to form as Widmanstätten and the presence of nitrides is hardly observed Fig.3. With a slower cooling rate the samples FA1 and F1 forming the austenite was more pronounced since there was enough time for dissolution of ferrite to austenite occurs and are formed in defined shape with equiaxial grains as shown in Fig.4 and Fig.5.

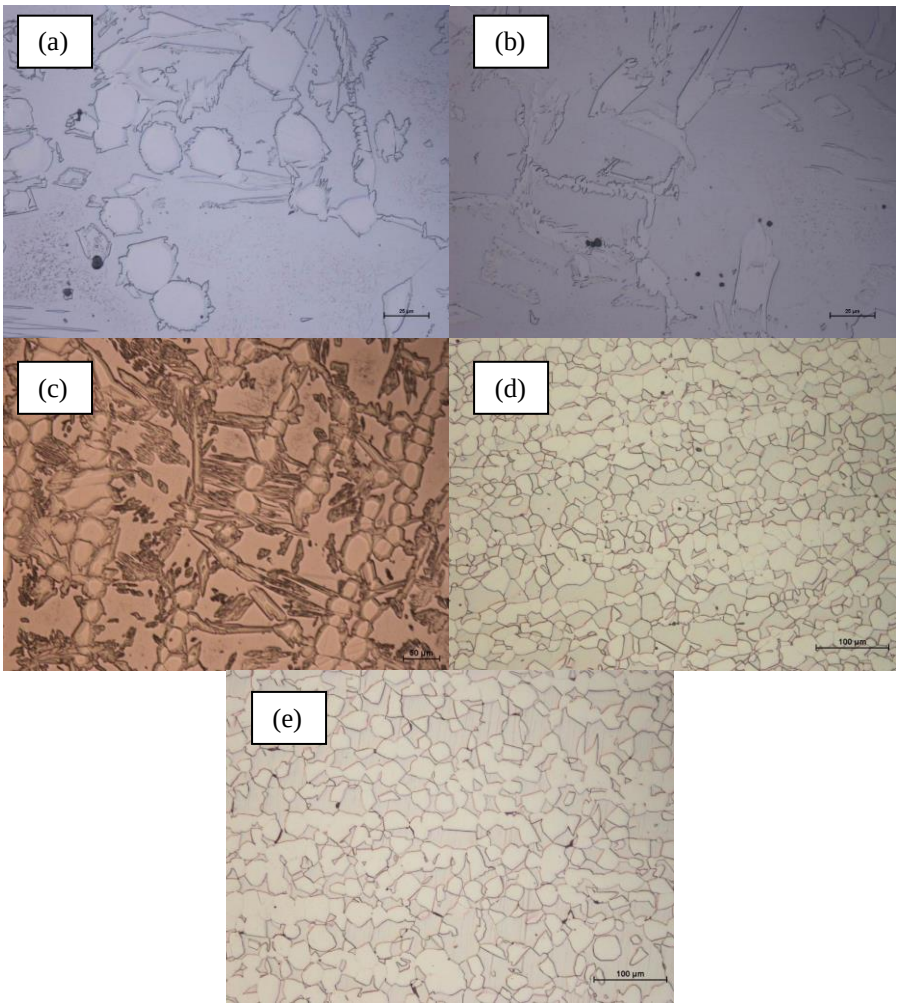

Figure 1. Micrographs of the samples (a) W1 (b) O1 (c) A1 (d) FA1 (e) F1 all attacked with 10% oxalic 3V 180s

W1 and O1 samples as the amount of austenite formed is far from the equilibrium value due to higher heating to 1100 ° C and fast cooling temperatures, almost all the nitrogen appears in the form of precipitates in ferrite sites (MARTINS; CASTELETTI, 2009).

During cooling, there is a competition between the precipitation of austenite and chromium nitride. The DSS retains almost all nitrogen in solid solution in austenite due to the solubility of N in this phase higher than in ferrite (BETTINI et al., 2013). The austenite begins to precipitate in the ferrite grain boundary. The amount of austenite formed is a

function of time and temperature, a higher volume fraction of austenite is obtained in lower cooling rates (SEDRIKS, 1996). Quenching with water to room temperature retains the ferrite phase (α) supersaturated and the alloy became susceptible to precipitation of deleterious phases when aged by reheating in the interface region α + γ (SOLOMON, 1983).

Samples from Series 2 were first submitted to the same heat treatment as Series 1, then exposed to 1000 °C for 1 h, and cooled in water. Austenite begins to form at temperatures lower than 1100 °C from the dissolution of ferrite. This annealing treatment is intended to equalize the phases present and the dissolution of intermetallic phases such as chromium nitrides Cr2N e CrN (RIBEIRO; SANTOS, 2009).

The O2 and W2 samples present a different structure of their predecessors W1 and O2, the amount of austenite increased, furthermore, the precipitates present were partially dissolved. The austenite was formed in lamellar shape in the interior of ferrite grains and in island shapes elongated in the grain boundary, making the grain size be decreased. Figure 7 can be seen that the austenite grains is larger and a presence of a distinct phase during dissolution □ → □, □2 may have been formed, this because the samples before annealing heat treatment had chrome nitrides and the ferrite formation mechanism is different in the presence of these precipitates (RAMIREZ et al., 2003).

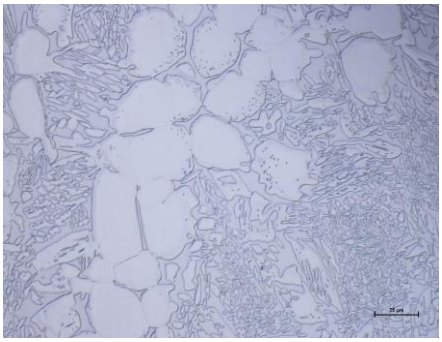

Figure 2. Sample micrograph W2 attacked with 10% oxalic 3V 180s

The duplex stainless steel UNS S31803 is considered susceptible to intergranular corrosion when the ratio (Ir/Ia) is greater than 5.00E-02 (LOPEZ et al., 1997) . This relationship was observed only in samples W1 as shown in Table 4.

Table 4 - Relationship Ir/Ia 1 series of samples tested by DL-EPR

Sample	Ir/Ia	SD
W1	5,13E-02	8,76E-03
O1	1,50E-02	1,92E-03
A1	7,66E-03	1,79E-03
FA1	9,56E-03	3,11E-03
F1	1,29E-02	8,16E-04

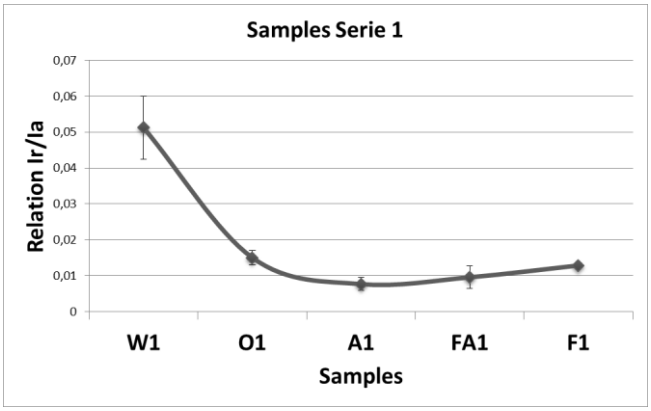

Figure 3. Comparison between samples Series 1 DL-EPR

Figure 8 illustrates the double-loop test for sample W1. All tests showed a potential slope near -300 mVSCE indicated by the red arrow because the fact of the presence of two ferrite phase and austenite. Only the sample W1 presented a significantly reactivation peak current Ir with a potential between -300 mVSCE and -200 mVSCE, indicating that the other samples were not susceptible to intergranular corrosion. The arrows in black indicate the direction of the sweep.

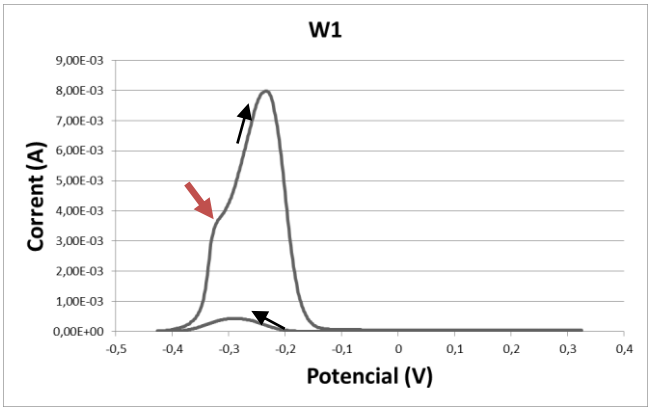

Figure 4. W1 Sample tested with solution presented corrent of Ia and Ir.

It was expected the annealing heat treatment the nitrides present in the samples be dissolved. With the annealing heat treatment on samples that had previously nitrides in the ferrite phase, they tend to dissolve and secondary austenite be precipitates which is a phase which can be nucleated in inclusions present in the material (RAMIREZ et al., 2003). The presence of the secondary austenite increases the hardness of the material as it was noted by (TAVARES et al., 2005) in his work, but its chemical composition affect the corrosion resistance.

Table 2 - Ratio Ir / Ia series of 2 samples tested by DL-EPR

Sample	Ir/Ia	SD
W2	1,01E-01	1,44E-02
O2	5,05E-02	1,60E-02
A2	8,29E-03	4,68E-03
FA2	5,27E-03	1,73E-03
F2	5,45E-03	2,55E-04

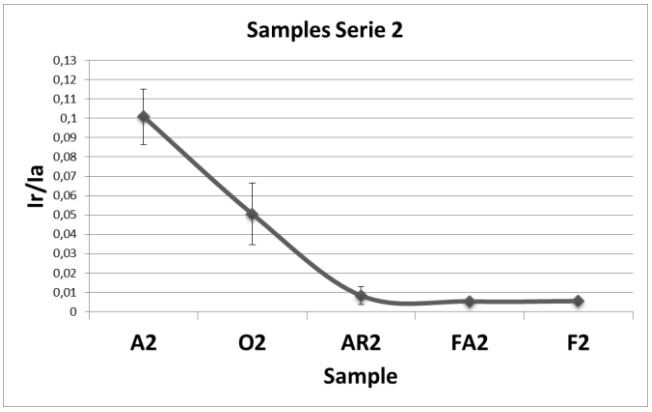

Figure 5. Comparison between samples Series 2 DL-EPR

When compared the samples before and after thermal annealing treatment, the samples W (water-cooled) and the (cooled oil) to pass through the annealing treatment had a higher degree of sensitization, the fact that it mainly during phase transformation $\alpha \rightarrow \gamma$, nitrides that existed in the samples served as the nucleation sites for $\gamma 2$. (RAMÍREZ LONDOÑO, 2002). Samples A remained with the same degree of sensitization, as the FA samples and F tend to have

lower due to more time for formation of austenite appropriately, since these samples did not have in its microstructure a ferritic phase supersaturated league elements.

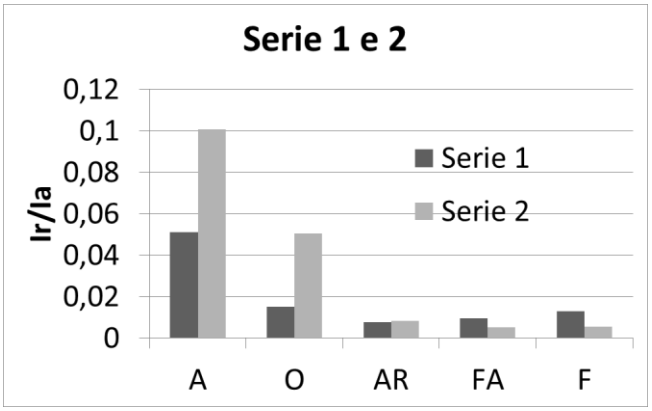

Figure 6. Sensitization (Ir / Ia) samples series 1 and 2

The sample W2 Figure 11 and O2 Figure 12 show the presence of nitrides and the high quantity of ferrite these samples had prior to the annealing heat treatment caused the precipitation of a phase that was not presented before in the samples. This phase was responsible for the increased susceptibility to intergranular corrosion of the samples relative to the previously.

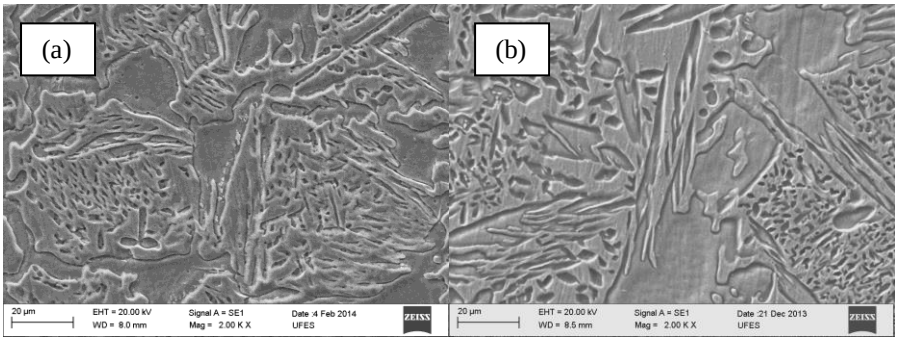

Figure 7. Micrographs samples after the test SEM DL-EPR (a) W2 (b) O2

A first analysis can be made by relating volume fraction of austenite and pitting potential Fig. 13. Smaller Epite values were presented by samples with higher fractions of austenite FA and F. Now, for fractions below 40%, an increased amount of austenite led to a slight increase in pitting potential. These results suggest that the amount of austenite by itself is not sufficient to increase the resistance to pitting corrosion. The balance between this phase and the fraction in the presence of reasonable amounts of the same elements as Cr, Mo and N, it is more important.

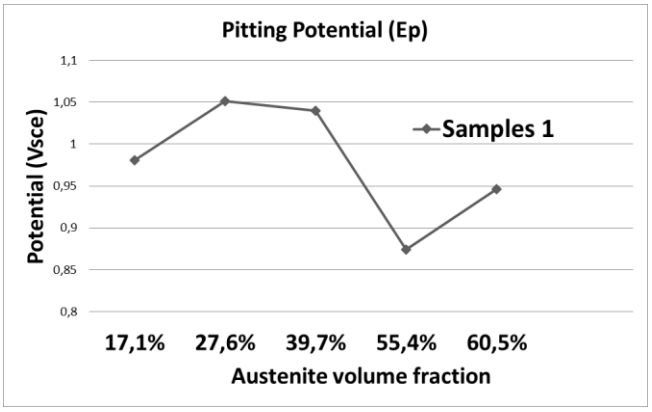

Figure 8. Pite relationship between potential and Volumetric fraction of Austenite (%)

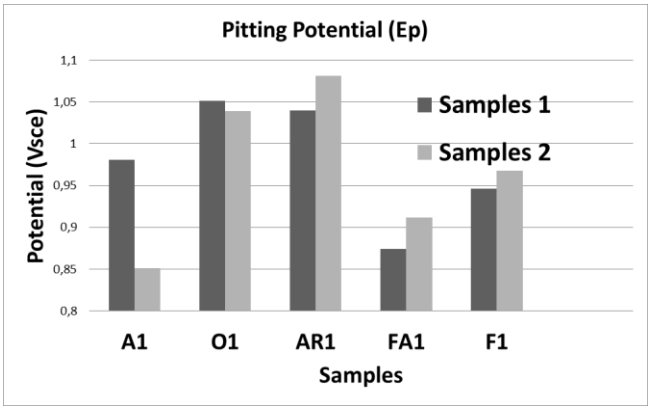

Figure 9. Comparative pitting potential between series 1 and 2 of each samples

The annealing treatment reduced the Epite from cooled sample in water W2 which that the sample has the lowest pitting potential (130 mV reduction) observed, as seen in Fig. 14. The highest values were obtained by cooled samples in air and oil. To the cooled sample in air, there was a increase in the pitting potential (40 mV) while no significant change to the cooled oil (12 mV). The pitting potential increased on average by 30 mV after solubilization (aging) for cooled samples in the oven. As the annealing produced equal amounts of austenite, the difference of the pitting potential depends of other phases precipitation and the alloy element contents dissolved in the austenite formed. The low amount of alloying elements present in the austenite may be the cause of increased susceptibility and pitting corrosion that phase with respect to ferrite (BETTINI et al., 2013).

4. CONCLUSIONS

Despite DSS UNS S31803 have a high corrosion resistance an inadequate thermal processing conditions may lead to a decrease of their properties

For OM and SEM micrographs in can be seen that for the treatment in elevated temperature faster cooling rates caused the formation of precipitates within the ferrite grains.

During the annealing heat treatment of the austenite formation mechanism in regions containing a high content of alloying elements may cause the precipitation of deleterious phases being a site of nucleation.

In the DL-EPR test it was observed that the presence of precipitated phases during the solubilization treatment resulted in increased susceptibility to intergranular corrosion in samples cooled in oil, and water. The solubilization treatment increased sensitization in cooled samples into oil and water.

Samples cooled in oven had lower pitting potential before and after aging. As for the water cooled condition, there was a reduction in the pitting potential after aging. The larger pitting potential were obtained for the samples cooled in oil and air.

5. ACKNOWLEDGEMENTS

The authors would like to acknowledge the Braziliam research agencies CNPq, PRH-29 and IFES for financial support.

6. REFERENCES

ASTM. ASTM G61 - 86 Standard Test Method for Conducting Cyclic Potentiodynamic Polarization Measurements for Localized Corrosion Susceptibility of Iron , Nickel , or Cobalt Based Alloys. , 2003.

BETTINI, E.; KIVISÄKK, U.; LEYGRAF, C.; PAN, J. Study of corrosion behavior of a 22% Cr duplex stainless steel: Influence of nano-sized chromium nitrides and exposure temperature. Electrochimica Acta, v. 113, p. 280–289, 2013.

COBB, H. M. The History of Stainless Steel. 2010.

GHOSH, S. K.; MONDAL, S. High temperature ageing behaviour of a duplex stainless steel. Materials Characterization, v. 59, n. 12, p. 1776–1783, 2008. Elsevier Inc.

LOPEZ, N.; CID, M.; PUIGGALI, M.; AZKARATE, I.; PELAYO, A. Application of double loop electrochemical potentiodynamic reactivation test to austenitic and duplex stainless steels. Materials Science and Engineering: A, v. 229, n. 1-2, p. 123–128, 1997.

MARTINS, M.; CASTELETTI, L. C. Microstructural characteristics and corrosion behavior of a super duplex stainless steel casting. Materials Characterization, v. 60, n. 2, p. 150–155, 2009..

PARDAL, J. M.; TAVARES, S. S. M.; PONZIO, E. A.; SCHMITT, V. M. Uma Revisão da Resistência à Corrosão em Aços Inoxidáveis Duplex e Superduplex. Revista Virtual de Química, 2013.

POHL, M.; STORZ, O.; GLOGOWSKI, T. Effect of intermetallic precipitations on the properties of duplex stainless steel. Materials Characterization, v. 58, n. 1, p. 65–71, 2007.

RAMIREZ, A. J.; LIPPOLD, J. C.; BRANDI, S. D. The relationship between chromium nitride and secondary austenite precipitation in duplex stainless steels. Metallurgical and Materials Transactions A, v. 34, n. 8, p. 1575–1597, 2003.

RAMÍREZ LONDOÑO, A. J. Intermetallic phases and secondary austenite precipitation at the multipass welding HAZ of duplex stainless steels. , 24. Oct. 2002. Universidade de São Paulo.

RIBEIRO, F. A.; SANTOS, H. Modificações da composição química do aço inoxidável duplex vazado 25Cr-6Ni-3Mo-3Cu para melhoria da resistência à corrosão por picadas. Ciência & Tecnologia dos Materiais, v. 21, n. 1-2, p. 68–83, 2009. Sociedade Portuguesa de Materiais.

SEDRIKS, A. J. Corrosion of stainless steels. 2nd ed. 1996.

SOLOMON, H. D. Age hardening in a duplex stainless steel. Journal of Heat Treating, v. 3, n. 1, p. 3–15, 1983. Springer-Verlag.

TAVARES, S. S. M.; TERRA, V. F.; PARDAL, J. M.; FONSECA, M. P. C. Influence of the microstructure on the toughness of a duplex stainless steel UNS S31803. Journal of Materials Science, v. 40, n. 1, p. 145–154, 2005.

VIJAYALAKSHMI, K.; MUTHUPANDI, V.; JAYACHITRA, R. Influence of heat treatment on the microstructure, ultrasonic attenuation and hardness of SAF 2205 duplex stainless steel. Materials Science and Engineering: A, v. 529, p. 447–451, 2011. Elsevier B.V.